Ceramics International **24** (1998) 605–609

PII: S0272-8842(97)00063-1
0272-8842/98 $19.00 + .00

Microstructures in 3D Carbon–Carbon Composites

Pu Tianyou[a] & Peng Weizhou[b]

[a]Beijing Center of Physical & Chemical Analysis, PO Box 8106, Beijing, China
[b]Beijing Research Institute of Materials & Technology, PO Box 9211, Beijing, China

(Received 7 February 1996; accepted 7 July 1997)

Abstract: Microstructures were studied of 3D carbon–carbon composites prepared by two different processes. Emphasis was given to microstructures and defects within the fibre/matrix interface region. © 1998 Published by Elsevier Science Limited and Techna S.r.l.

1 INTRODUCTION

3D carbon–carbon composites are multi-phase systems, with 3D woven billets as reinforcement and different combinations of deposited carbon (CVD carbon), pitch carbon and resin transformed carbon (resin carbon) as matrix and their matrix structures are directly dependent upon matrix selection and fabrication process. The composites show great complexity in microstructure, which has been the subject of concerted research.[1,2]

Different microscopic instruments are necessary for observation of microstructures in 3D carbon–carbon composites at different levels: the optical microscope may be used to obtain a general view of the internal structure and crystallographic features can be revealed if polarised light is utilised; the scanning electron microscopy (SEM) may be employed to observe fractured surfaces, ablated surfaces and polished metallographic surfaces; the transmission electron microscopy (TEM) may provide insight into finer structures at nanometer scale, especially microstructures within the interface region.

This paper presents results of research by SEM and TEM in microstructural features of 3D carbon–carbon composites.

2 EXPERIMENTAL

2.1 Material preparation

Two different processes were adopted for preparation of the carbon–carbon composites. The reinforcing billets were woven with PAN-based carbon fibres, with bundle spacing ranging from 0.5 mm to 0.7 mm and X–Y–Z yarn numbers being 2, 2 and 3, respectively.

Matrix composition and preparation processes of the two carbon–carbon composites are listed in Table 1.

2.2 Experimental procedure

Gold was sputtered on ablated surfaces for SEM observation. An accelerating voltage of 25 KV was chosen.

Preparation of TEM specimens involved ultra microtome cutting and ion bombarding. The accelerating voltage was 200 KV.

3 RESULTS AND DISCUSSION

3.1 Results

Results from TEM and SEM observations for the two sets of samples are separately given below.

3.1.1 Material no. 1

Figures 1 and 2 show the matrix structure within fibre bundles. CVD carbon is seen around single filaments. And the CVD carbon apparently falls into two layers: the inner layer is a dense layer of fine carbon granules and it is approximately 0.5 μm in thickness; the outer layer is more graphitic and circumferentially aligned lamellae are evident, with

Table 1. Matrix composition and preparation process

Designation	Preparation process	Matrix composition
No. 1	(1) CVD treatment of billet (2) Multi-cycles of resin impregnation and carbonisation (3) Graphitisation	CVD carbon Resin carbon
No. 2	(1) Slight CVD treatment of billet (2) Multi-cycles of HPIC (3) Graphitisation	CVD carbon Pitch carbon

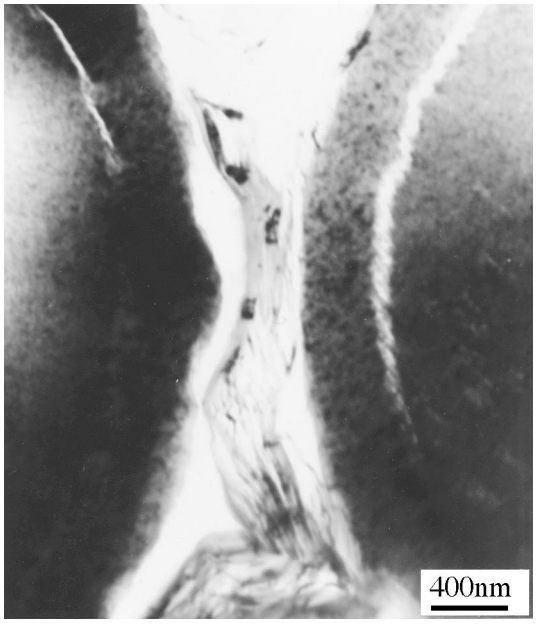

Fig. 1. TEM micrograph of matrix carbon within bundles.

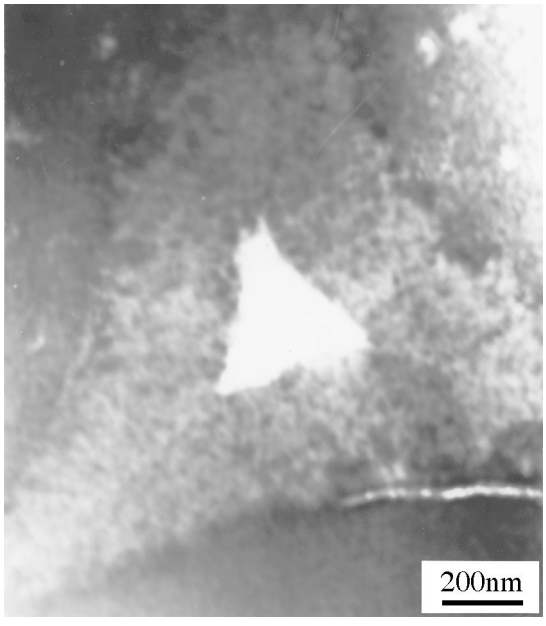

Fig. 2. Lamellar CVD carbon within the dense CVD carbon.

thickness ranging from 0.2 μm to 1 μm and distribution being non-uniform. The inter-filament regions are generally filled with resin carbon, but regions also exist where resin carbon is absent and losed cavities appear.

In some regions, lamellar CVD carbon exists between the dense CVD carbon layer and the fibre surface, see Fig. 3. And, as shown in Fig. 4, circular disclinations appear at defects on the fibre surface.

CVD carbon around the bundles appear similar to CVD carbon around single filaments, consisting

Fig. 3. Lamellar CVD carbon between the dense CVD carbon and the fibre surface.

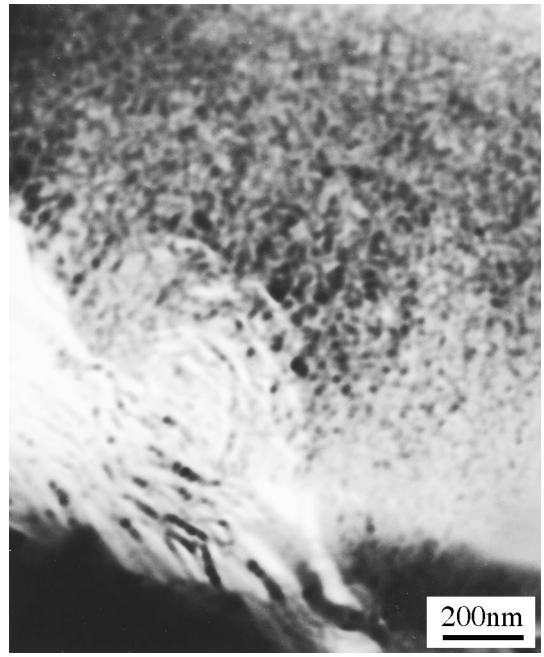

Fig. 4. Disclination of lamellar CVD carbon at a fibre surface defect.

of a dense inner layer and an oriented lamellar outer layer.

Many interfacial gaps exist between the CVD carbon and the filaments, and gaps also appear in the interface region the dense inner layer and the oriented lamellar outer layer. In addition, other types of defects also exist.

The microstructures illustrated above have direct influence on ablation performance. Figures 5 and 6 are SEM micrographs of ablated surfaces. It can be seen from the micrographs that the carbon fibres and the carbon matrix underwent non-uniform ablation. The lamellar CVD carbon was preferentially ablated and the dense CVD carbon layer showed greater resistance to ablation; the carbon fibres experienced preferential ablation along the interface, showing cone-shaped fibre ends; mechanical denudation occurred for the carbon fibres and the lamellar CVD carbon layer; interfacial gaps between the CVD carbon and carbon fibres extended during ablation.

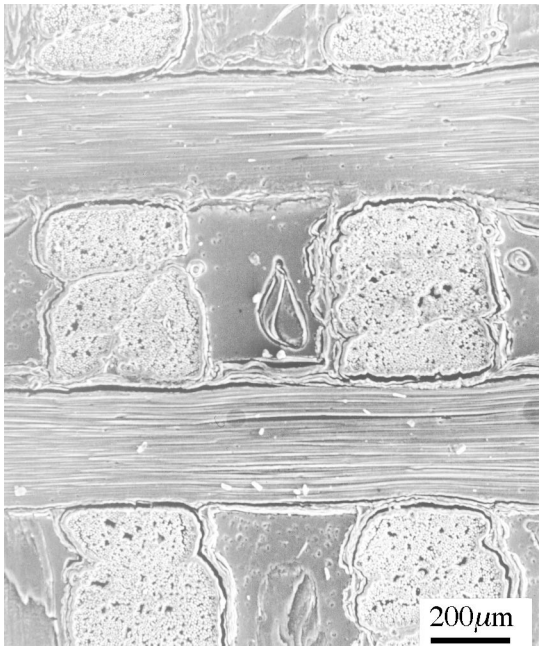

Fig. 5. SEM micrograph of material no. 1.

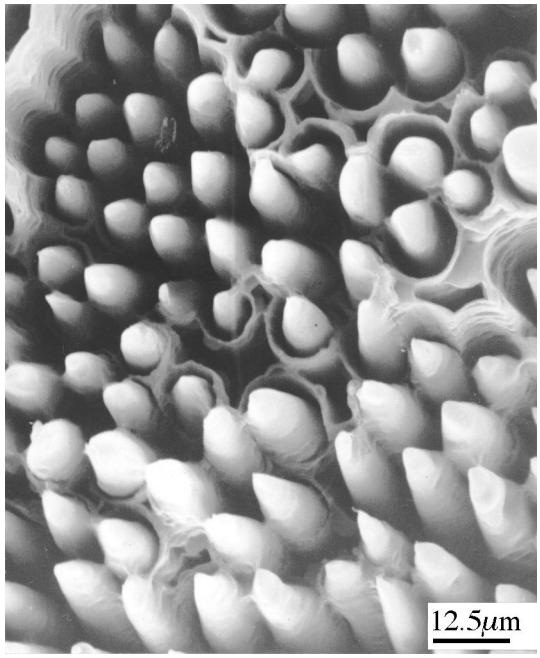

Fig. 6. Z–direction bundles preferentially ablated along the interface. The lamellar CVD carbon was preferentially ablated.

Slightly ablated fibre cross-sections show characteristic of radial alignment.

3.1.2 Material no. 2

Figures 7–10 are TEM micrographs showing the microstructural features in material no. 2. It can be seen that the PAN-based carbon fibres experienced significant microstructural change during composite fabrication, especially high temperature graphitization, and the changes revealed include radial alignment of outer microcrystals, alternation of radial and circumferential alignments and etc. The CVD carbon layer on the fibre surface appears very thin, and is non-uniform in thickness, ranging from 10 nm to 100 nm. And, microcrystals in the CVD carbon form an inter-penetrating cross-linked network (IPCN). Inter-filament pitch carbon lamellae show cross-linked structure, and differently aligned lamellar orientations exist in addition to the transversely aligned orientation.

Multiple interfacial structures exist in the material which include 'pinning structure' region between CVD carbon and fibre surfare, mechanical bonding region, interfacial gaps, 'induced structure' region between CVD carbon and pitch carbon, and interfacial defects region.

Figures 11 and 12 are SEM micrographs of ablated surfaces. The micrographs show comparatively

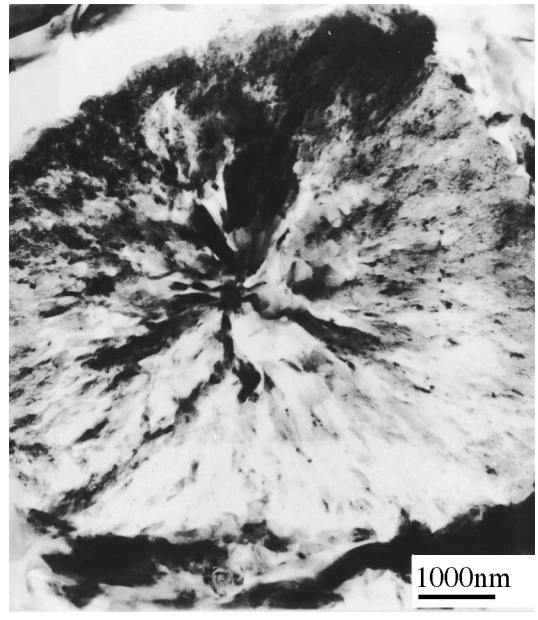

Fig. 7. Micro-texture of fibre cross-section.

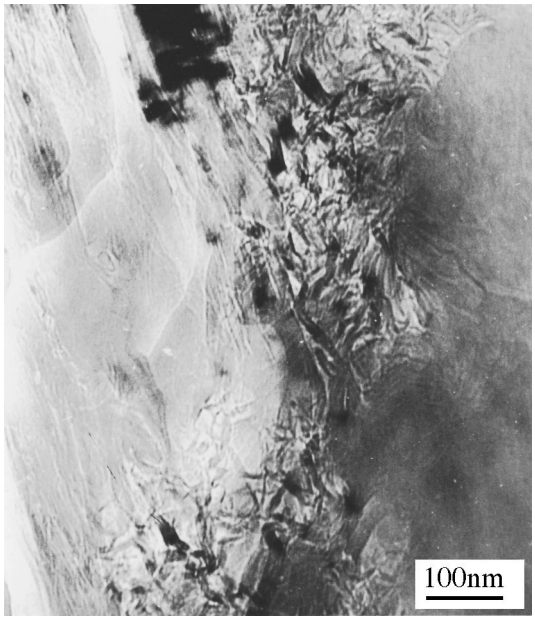

Fig. 8. Non-uniform distribution of CVD carbon on the fibre surface.

Fig. 10. Orientation of cross-linked lamellar pitch carbon between single filaments.

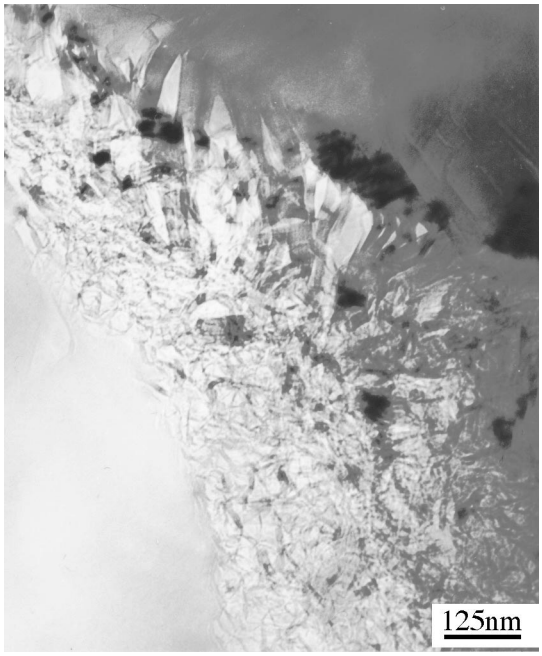

Fig. 9. Interface region between CVD carbon and pitch carbon.

Fig. 11. SEM micrograph of ablated surface from material no. 2.

uniform ablation. Cracks around the bundles propogated during ablation, the lamellar structure of pitch carbon was revealed an pitch carbon within the bundles was preferentially ablated. Ablated fibre cross-sections show apparent radial alignment.

3.2 Discussion

The two 3D carbon–carbon composites show considerable difference in microstructure and ablation performance. In view of ablation performance, material no. 2 is superior to material no. 1.

More inferfacial gaps exist in material No. 1 and, the lumpy resin carbon and lamellar CVD carbon layer are vulnerable to denudation. Whereas, less interfacial gaps exist in material no. 2 and the lamellor pitch carbon is cross-linked and highly graphitised and is thus move resistant to thermal shock and ablation. In addition, material no. 2 has a thinner CVD carbon layer which serves as a transitional region between the carbon fibres and

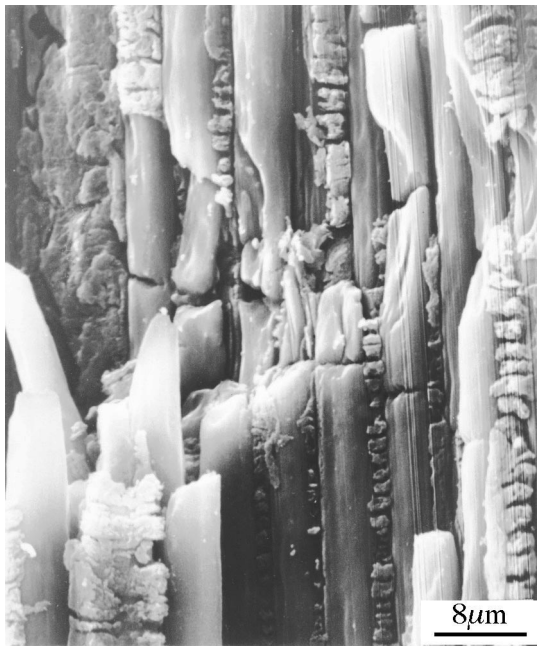

Fig. 12. Orientation of lamellar pitch carbon within fibre bundle.

the pitch carbon, forming a 'pinning structure' region with the fibre surface and an 'induced structure' region with the pitch carbon. Thermal shock resistance is thus enhanced.

CVD carbon in material no. 1 is comparatively thick and falls into two distinct layers. Many interfacial gaps exist in the interfaces between the two CVD layers, the dense CVD carbon and the fibre surface and, the CVD carbon and resin carbon. These gaps are the result of mismatch in thermal expansion coefficient of carbon fibres, CVD carbon and resin carbon. And, the gaps have adverse effect on ablation performance.

4 CONCLUSION

TEM can reveal microstructures in 3D carbon–carbon composites at nanometer scale, especially microstructure of the interface, and SEM observation on ablated surfaces can provide information about the ablation behaviour of discrete phases (fibre, matrix, interface). Therefore, combined use of TEM and SEM may relate ablation performance to material microstructure.

Observation of material no. 1 and material no. 2 defined difference in their microstructure and, the difference was correlated to difference in ablation behavior. Results show that the existence of interfacial defects. lumpy glassy carbon and lamellar CVD carbon is unfavourable for ablation resistance.

ACKNOWLEDGEMENT

Financial support by the National Natural Sciences Foundation of China is gratefully acknowledged.

REFERENCES

1. PENG WEIZHOU, PU TIANYOU, ZENG HANMIN & YU QIAO, In *Interfaces in Polymer, Ceramic and Metal Matrix Composites*, ed. H. Ishida. Elsevier, New York, 1988, pp. 399–411.
2. PENG WEIZHOU, YU QUAO, ZENG HANMIN & PU TIANYOU, In *ICCM Proceedings of The Seventh International Conference on Composite Materials*, Volume 3, Guang Zhou, China, 1989, pp. 559–563.